

Status of the Muon Anomalous Magnetic Moment

Eduardo de Rafael^{*†}

Centre de Physique Théorique, CNRS-Luminy, Case 907, F-13288 Marseille Cedex 9, France ‡

E-mail: EdeR@cpt.univ-mrs.fr

These pages, based on my talk at the Valencia *International Workshop on Effective Field Theories: from the pion to the epsilon*, provide us with a short update of the Standard Model contributions to the muon anomalous magnetic moment.

International Workshop on Effective Field Theories: from the pion to the epsilon
February 2-6 2009
Valencia, Spain

*Speaker.

†This work has been supported in part by the EU RTN network FLAVIANet [Contract No. MRTN-CT-2006-035482]. The author is grateful to Jean-Philippe Aguilar, David Greynat, Marc Knecht, Joaquim Prades and Arkady Vainshtein for helpful discussions.

‡Unité Mixte de Recherche (UMR 6207) du CNRS et des Universités Aix-Marseille 1, Aix-Marseille 2 et sud Toulon-Var, affiliée à la FRUMAN.

Preprint: CPT-P037-2009.

1. Introduction

We shall be concerned with the g -factor of the muon which relates its spin \vec{s} to its magnetic moment $\vec{\mu}$:

$$\vec{\mu} = g_\mu \frac{e\hbar}{2m_\mu c} \vec{s}, \quad \underbrace{g_\mu = 2(1 + a_\mu)}_{\text{Dirac}}; \quad (1.1)$$

more precisely, with the correction a_μ to the Dirac value $g_\mu = 2$, i.e. the correction which generates the so called anomalous magnetic moment. The present experimental world average determination, which is dominated by the latest BNL experiment (the E821 collaboration [1]), is

$$a_\mu^{\text{exp}} = 116\,592\,080(63) \times 10^{-11} (0.54 \text{ ppm}), \quad (1.2)$$

where the origin of the error is 0.46 ppm statistical and 0.28 ppm systematic. This determination assumes CPT-invariance i.e., $a_{\mu^-} = a_{\mu^+}$.

The question we shall discuss is: *how well can the Standard Model digest this precise number?* As we shall see, the precision of a_μ^{exp} is such that it is sensitive to the three couplings of the Gauge Theory which defines the Standard Model, as well as to its full particle content ¹.

2. The QED Contributions (Leptons)

This is by far the dominant contribution, which is generated by two types of Feynman diagrams:

2.1 The Massless Class

This class consists of Feynman diagrams with virtual photons only as well as diagrams with virtual photons and fermion loops of the same flavour as the external particle (the muon in our case). Since the anomalous magnetic moment is a dimensionless quantity, this class of diagrams gives rise to a contribution which is the same for the muon, the electron and the tau anomalies. It corresponds to the entries $a^{(2n)}$ in Table 1, with $n = 1, 2, 3, 4$ indicating the number of loops involved. They are known analytically at one loop [4]; two loops [5, 6]; and three loops [7]. This is the reason why there is no error in the corresponding numbers in the second column of Table 1.

At the four-loop level, there are 891 Feynman diagrams of this type. Some of them are already known analytically, but in general one has to resort to numerical methods for a complete evaluation. This impressive calculation, which is systematically pursued by Kinoshita and collaborators, requires many technical skills and is under constant updating; in particular thanks to the advances in computing technology. The entry $a^{(8)}$ in Table 1 is the one corresponding to the most recent published value [8], with the error due to the present numerical uncertainties.

Notice the alternating sign of the results from the contributions of one loop to four loops, a simple feature which is not yet *a priori* understood. Also, the fact that the sizes of the $(\frac{\alpha}{\pi})^n$ coefficients for $n = 1, 2, 3, 4$ remain rather small is interesting, allowing one to expect that the order of magnitude of the five-loop contribution, from a total of 12 672 Feynman diagrams, is likely to

¹For recent review articles see e.g. refs. [2] and [3].

Table 1: QED Contributions (Leptons) $\{\alpha^{-1} = 137.035\,999\,084\,(51)\,[0.37\text{ ppb}]\}$

CONTRIBUTION	RESULT IN POWERS OF $\frac{\alpha}{\pi}$	NUMERICAL VALUE IN 10^{-11} UNITS
$a_\mu^{(2)}$	$0.5\left(\frac{\alpha}{\pi}\right)$	116 140 973.29 (0.04)
$a_\mu^{(4)}$ $a_\mu^{(4)}(m_\mu/m_e)$ $a_\mu^{(4)}(m_\mu/m_\tau)$ $a_\mu^{(4)}(\text{total})$	$-0.328\,478\,965\,(00)\left(\frac{\alpha}{\pi}\right)^2$ $1.094\,258\,311\,(08)\left(\frac{\alpha}{\pi}\right)^2$ $0.000\,078\,064\,(26)\left(\frac{\alpha}{\pi}\right)^2$ $0.765\,857\,410\,(27)\left(\frac{\alpha}{\pi}\right)^2$	413 217.62 (0.01)
$a_\mu^{(6)}$ $a_\mu^{(6)}(m_\mu/m_e)_{\text{vp}}$ $a_\mu^{(6)}(m_\mu/m_\tau)_{\text{vp}}$ $a_\mu^{(6)}(m_\mu/m_e, m_\mu/m_\tau)_{\text{vp}}$ $a_\mu^{(6)}(m_\mu/m_e)_{ \text{x} }$ $a_\mu^{(6)}(m_\mu/m_\tau)_{ \text{x} }$ $a_\mu^{(6)}(\text{total})$	$1.181\,241\,46\,(00)\left(\frac{\alpha}{\pi}\right)^3$ $1.920\,455\,13\,(03)\left(\frac{\alpha}{\pi}\right)^3$ $-0.001\,782\,33\,(48)\left(\frac{\alpha}{\pi}\right)^3$ $0.000\,527\,66\,(17)\left(\frac{\alpha}{\pi}\right)^3$ $20.947\,924\,89\,(16)\left(\frac{\alpha}{\pi}\right)^3$ $0.002\,142\,83\,(69)\left(\frac{\alpha}{\pi}\right)^3$ $24.050\,509\,64\,(43)\left(\frac{\alpha}{\pi}\right)^3$	30 141.90 (0.00)
$a_\mu^{(8)}$ $a_\mu^{(8)}(m_\mu/m_e)_{\text{vp}}$ $a_\mu^{(8)}(m_\mu/m_e, m_\mu/m_\tau)_{\text{vp}}$ $a_\mu^{(8)}(m_\mu/m_e)_{ \text{x} }$ $a_\mu^{(8)}(m_\mu/m_e, m_\mu/m_\tau)_{ \text{x} }$ $a_\mu^{(8)}(\text{total})$	$-1.914\,4\,(35)\left(\frac{\alpha}{\pi}\right)^4$ $10.839\,2\,(41)\left(\frac{\alpha}{\pi}\right)^4$ $-0.046\,2\,(00)\left(\frac{\alpha}{\pi}\right)^4$ $121.843\,1\,(59)\left(\frac{\alpha}{\pi}\right)^4$ $0.083\,8\,(01)\left(\frac{\alpha}{\pi}\right)^4$ $130.805\,5\,(80)\left(\frac{\alpha}{\pi}\right)^4$	381.33 (0.02)
$a_\mu^{(10)}(\text{total estimate})$	$663\,(20)\left(\frac{\alpha}{\pi}\right)^5$	4.48 (0.14)
$a_\mu^{(2+4+6+8+10)}(\text{QED})$		116 584 718.09 (0.14)(0.04)

be of $\mathcal{O}(\alpha/\pi)^5 \simeq 7 \times 10^{-14}$. This is well beyond the accuracy required to compare with the present experimental result for a_μ , but it will be eventually needed for an improved determination of the fine-structure constant α from the precision measurements of the electron anomaly. The value of α used in Table 1 is the one quoted in ref. [9].

2.2 The Massive Class

This second class is generated by Feynman diagrams with lepton loops of a different flavour to

POS(EFT09)050

the one of the external muon line. Their contribution to a_μ is then a function of the ratios of lepton masses involved. The relevant diagrams are those generated by vacuum polarization subgraphs (vp) and/or by light-by-light scattering subgraphs (lxl) involving electron and tau loops. The results of their evaluation are given in Table 1. Both the two-loop and three-loop contributions of this class are known analytically². The full three-loop evaluation involving electron-loop subgraphs, by Laporta and Remiddi [10, 11], is a remarkable achievement. The numerical errors quoted in Table ?? tab:QED for these contributions are due to the present experimental errors in the lepton masses [12].

At the four-loop level, only a few contributions are known analytically. Kinoshita and his collaborators have, however, accomplished a full numerical evaluation of this class (see ref. [13] and references therein.). The corresponding error in Table 1 is the combined error in the lepton masses and the present error due to the very many integrals which have been performed numerically.

The number quoted for the full five-loop QED contribution in Table 1 is the present estimate quoted in ref. [14]. It is likely to be improved in the near future.

2.3 The Mellin–Barnes Technique

There has been a recent technical development in the evaluation of Feynman diagrams involving mass ratios, which has already been useful in the evaluation of some higher order contributions to a_μ (see refs. [15, 16]) and which seems promising for further calculations. In these papers it is shown how the Mellin–Barnes representation of Feynman parametric integrals allows for an easy evaluation of as many terms as wanted in the asymptotic expansion of Feynman diagrams in terms of one and two mass ratios.

The basic idea is to express the contribution to a_μ from a Feynman diagram, or a class of diagrams, as an inverse Mellin transform with respect to the mass ratios involved in the diagrams. The remarkable property of this representation is the factorization in terms of massless moment integrals. It is in fact this factorization which is at the origin of the well known renormalization group properties discussed in ref. [17], and used since then by many other authors (see e.g. ref. [18] and references therein). The algebraic factorization in the Mellin–Barnes representation, however, is more general. The standard renormalization group constraints only apply to the evaluation of asymptotic behaviours in terms of *powers of logarithms* and *constant* terms. In the Mellin–Barnes framework, these contributions are governed by the residues of the leading Mellin singularities. What is new here is the extension of the renormalization group predictive power to *subleading contributions* as well. They are in fact governed by the residues of the successive Mellin singularities (in the negative real axis, in the case of internal electron loops); or by two-dimensional residue forms [16, 19], in the case of the Mellin singularities associated to two mass ratios (i.e. in the case of both electron and tau internal loops).

As an example, we quote a few terms of the result obtained for the tenth-order contribution from the string of vacuum polarization subgraphs shown in Fig. 1:

²For an account of the successive improvements in the evaluation of these contributions see e.g. refs. [2, 3].

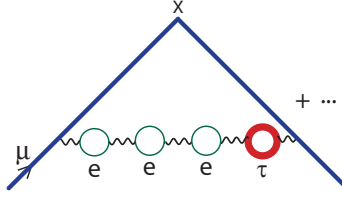


Fig.1 Diagrams with three e -loops and a τ -loop.

$$\begin{aligned}
 a_{\mu}^{(eee\tau)} &= \left(\frac{\alpha}{\pi}\right)^5 \left\{ \left(\frac{m_{\mu}^2}{m_{\tau}^2}\right) \left[\frac{4}{1215} \log^3 \frac{m_{\mu}^2}{m_e^2} - \frac{2}{405} \log^2 \frac{m_{\mu}^2}{m_e^2} - \left(\frac{122}{3645} - \frac{8\pi^2}{1215}\right) \log \frac{m_{\mu}^2}{m_e^2} + \frac{2269}{32805} - \frac{4\pi^2}{215} - \frac{16}{405} \zeta(3) \right] \right. \\
 &\quad \left. + \left(\frac{m_e^2}{m_{\tau}^2}\right) \left[\frac{4}{45} \log^2 \frac{m_{\mu}^2}{m_e^2} - \frac{20}{27} \log \frac{m_{\mu}^2}{m_e^2} + \frac{634}{405} + \frac{8\pi^2}{135} \right] + \dots \right\} \\
 &= \left(\frac{\alpha}{\pi}\right)^5 0.013\,057\,4(4).
 \end{aligned} \tag{2.1}$$

In fact, the analytic calculation in ref. [16] which leads to this precise number, also includes terms up to $\mathcal{O}\left[\left(\frac{m_{\mu}^2}{m_{\tau}^2}\right)^4 \log^3 \frac{m_{\mu}^2}{m_e^2}\right]$, which are already smaller than the error generated by the lepton masses in the leading order terms given in the first line in Eq. (2.1).

So far, the contributions to the muon anomaly evaluated analytically with this technique are: those from the two sixth order Feynman diagrams which give the contribution $a_{\mu}^{(6)}(m_{\mu}/m_e, m_{\mu}/m_{\tau})_{\text{vp}}$ in Table 1 [15]; those from the eighth and tenth order Feynman diagrams involving lowest order vacuum polarization insertions of leptons $l = e, \mu, \tau$ in the Schwinger lowest order graph [16]; and recently, those from the eighth order contributions involving fourth order vacuum polarization insertions of leptons also in the lowest order Schwinger graph [19, 20].

3. QED Hadronic Contributions

The electromagnetic interactions of hadrons produce contributions to a_{μ} induced by the hadronic vacuum polarization and by the hadronic light-by-light scattering.

3.1 Hadronic Vacuum Polarization

All calculations of the lowest-order hadronic vacuum polarization contribution to the muon anomaly (see Fig. 2) are based on the spectral representation [21]

$$a_{\mu}^{\text{hvp}} = \frac{\alpha}{\pi} \int_0^{\infty} \frac{dt}{t} \frac{1}{\pi} \text{Im}\Pi(t) \int_0^1 dx \frac{x^2(1-x)}{x^2 + \frac{t}{m_{\mu}^2}(1-x)} \tag{3.1}$$

with the hadronic spectral function $\frac{1}{\pi} \text{Im}\Pi(t)$ related to the *one-photon* e^+e^- annihilation cross-section into hadrons ($m_e \rightarrow 0$) as follows:

$$\sigma(t)_{\{e^+e^- \rightarrow (\gamma) \rightarrow \text{hadrons}\}} = \frac{4\pi^2\alpha}{t} \frac{1}{\pi} \text{Im}\Pi(t). \tag{3.2}$$

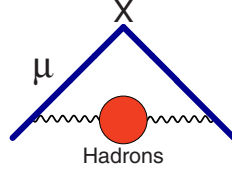


Fig.2 Hadronic Vacuum Polarization

This contribution is dominated by the $\pi^+\pi^-$ channel; the region of the ρ -resonance in particular [22, 23]. The history of evaluations of a_μ^{hvp} is a long one which can be traced back, e.g. in ref. [2]. The most recent compilation of e^+e^- annihilation data used in the evaluation of the dispersive integral in Eq. (3.1) made by Michel Davier and collaborators, which also includes the new precise measurements from the experiments SND and CMD-2 at Nobosibirsk, gives the result ³:

$$a_\mu^{\text{hvp}} = (6\,873 \pm 42_{\text{exp}} \pm 19_{\text{rad}} \pm 7_{\text{QCD}}) \times 10^{-11} \quad [e^+e^- \text{ - data}], \quad (3.3)$$

where the error $\pm 19_{\text{rad}}$ refers to uncertainties in the treatment of radiative corrections in some of the e^+e^- experiments.

The evaluation made using the τ -spectral functions gives, however, a much larger contribution ⁴:

$$a_\mu^{\text{hvp}} = (7\,015 \pm 48_{\text{exp+IB}} \pm 8_{\text{rad}} \pm 7_{\text{QCD}}) \times 10^{-11} \quad [\tau \text{ - data}]. \quad (3.4)$$

In spite of the corrections for isospin-breaking effects (IB), the discrepancy with the evaluation made using e^+e^- data, unfortunately, still persists. Here, one has to wait for the forthcoming results from the high precision measurements on the $\pi\pi$ mode at BaBar using the radiative return method. Hopefully, we shall then be able to resolve the inconsistency between the results in Eqs. (3.3) and (3.4) and, therefore, improve the accuracy of the a_μ^{hvp} contribution.

There is a similar spectral representation to the one in Eq. (3.1) for the next-to-leading order hadronic vacuum polarization [25], with the kernel [26, 27] in Eq. (3.1), replaced by a two-loop kernel, which is also known analytically [28]. A recent numerical evaluation, using the same data as for the lowest-order e^+e^- evaluation, gives [29]

$$a_\mu^{\text{hvp(nlo)}} = (-97.9 \pm 0.9_{\text{exp}} \pm 0.3_{\text{rad}}) \times 10^{-11}. \quad (3.5)$$

A simple explanation of why this contribution turns out to be negative is given in ref. [2].

3.2 Hadronic Light-by-Light Scattering

Unlike the hadronic vacuum polarization contribution, there is no direct experimental input for the hadronic light-by-light scattering contribution to a_μ shown in Fig. 3; therefore one has to rely on theoretical approaches.

So far, the only rigorous theoretical result is the observation that, in the QCD large- N_c limit and to leading order in the chiral expansion, the dominant contribution comes from the Goldstone-like neutral pion exchange which produces a characteristic universal double logarithmic behavior with a coefficient which can be calculated exactly [30]:

³See ref. [24] and references therein for details.

⁴See also ref. [24] and references therein for details.

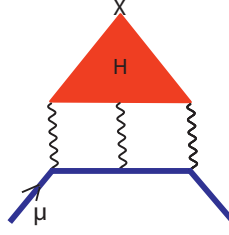


Fig.3 Hadronic Light-by-Light Scattering

$$a_{\mu}^{\text{hll}}(\pi^0) = \left(\frac{\alpha}{\pi}\right)^3 \frac{m_{\mu}^2 N_c^2}{48\pi^2 F_{\pi}^2} \left[\ln^2 \frac{m_{\rho}}{m_{\pi}} + \mathcal{O}\left(\ln \frac{m_{\rho}}{m_{\pi}}\right) + \mathcal{O}(1) \right] \quad (3.6)$$

where F_{π} denotes the pion coupling constant in the chiral limit ($F_{\pi} \sim 90$ MeV). Testing this limit was particularly useful in fixing the sign of the phenomenological calculations of the neutral pion exchange [31].

Although the coefficient of the $\ln^2(m_{\rho}/m_{\pi})$ term in Eq. (3.6) is unambiguous, the coefficient of the $\ln(m_{\rho}/m_{\pi})$ term depends on low-energy constants which are difficult to extract from experiment [30, 32] (they require a detailed knowledge of the $\pi^0 \rightarrow e^+e^-$ decay rate with inclusion of radiative corrections). Moreover, the constant term in Eq. (3.6) is not fixed by chiral symmetry requirements, which makes the predictive power of an effective chiral perturbation theory approach rather limited for our purposes. Therefore, one has to adopt a dynamical framework which takes into account explicitly the heavier meson degrees of freedom as well. This, at the present stage of our knowledge of QCD, necessarily brings in some model dependency.

The most recent calculations of a_{μ}^{hll} in the literature [31, 33, 34, 35] are all compatible with the QCD chiral constraints and large- N_c limit discussed above. They all incorporate the π^0 -exchange contribution modulated by $\pi^0 \gamma^* \gamma^*$ form factors, correctly normalized to the $\pi^0 \rightarrow \gamma\gamma$ decay width. They differ, however, in the shape of the form factors, originating in different assumptions: vector meson dominance in a specific form of Hidden Gauge Symmetry in Ref. [33]; in the form of the extended Nambu-Jona-Lasinio (ENJL) model in ref. [34]; large- N_c models in Refs. [31, 35]; and on whether or not they satisfy the particular operator product expansion constraint discussed in ref. [35].

The question of using on-shell form factors $\mathcal{F}_{\pi^0 \gamma^* \gamma^*}(m_{\pi}^2, q_1^2, q_2^2)$ versus off-shell form factors $\mathcal{F}_{\pi^0 \gamma^* \gamma^*}(q_3^2, q_1^2, q_2^2)$ has been recently raised again in ref. [36] (see also ref. [3]). In fact, one can show⁵ that these two choices are correlated with the treatment of the remaining contributions to the full a^{hll} . In a Lagrangian formulation of the problem, like e.g. within the ENJL-model, there are no such ambiguities.

In order to compare different results it is convenient to separate the hadronic light-by-light contributions which are leading in the $1/N_c$ -expansion from the non-leading ones [37]. Among the leading contributions, the pseudoscalar meson exchanges which incorporate the π^0 , and to a lesser degree the η and η' exchanges, are the dominant ones. As discussed above, there are good QCD theoretical reasons for that. In spite of the different definitions of the pseudoscalar meson exchanges and the associated choices of the form factors used in the various model calculations, there is a reasonable agreement among the final results. The result quoted in a recent update

⁵Marc Knecht unpublished notes.

discussed in ref. [38] gives:

$$a^{\text{hll}}(\pi, \eta, \eta') = (114 \pm 13) \times 10^{-11}. \quad (3.7)$$

Other contributions, which are also leading in the $1/N_c$ -expansion, due to axial-vector exchanges and scalar exchanges, give smaller contributions with updated errors, as discussed in ref. [38]:

$$a^{\text{hll}}(1^+) = (15 \pm 10) \times 10^{-11}, \quad (3.8)$$

and

$$a^{\text{hll}}(0^+) = -(7 \pm 7) \times 10^{-11}. \quad (3.9)$$

The subleading contributions in the $1/N_c$ -expansion are dominated by the charged pion loop. However, because of the model dependence of the results one obtains when the pion loop is dressed with hadronic interactions it is suggested in ref. [38] to use the central value of the ENJL-model evaluation in [34], but with a larger error which also covers unaccounted loops of other mesons, :

$$a^{\text{hll}}(\pi^+ \pi^-) = -(19 \pm 19) \times 10^{-11}. \quad (3.10)$$

From these considerations, adding the errors in quadrature, as well as the small charm contribution: $a^{\text{hll}}(c) = 2.3 \pm \times 10^{-11}$, one gets

$$a^{\text{hll}} = (105 \pm 26) \times 10^{-11}, \quad (3.11)$$

as a final estimate.

4. Electroweak Contributions

The leading contribution to a_μ from the Electroweak Lagrangian of the Standard Model, originates at the one-loop level. The relevant Feynman diagrams (in the unitary gauge) are shown in Fig. 4.

The analytic evaluation of the overall contribution gives the result (see e.g. ref. [39]):

$$a_\mu^{\text{EW}(1)} = \frac{G_F m_\mu^2}{\sqrt{2} 8\pi^2} \left\{ \underbrace{\frac{10}{3}}_W + \underbrace{\frac{1}{3}(1-4\sin^2\theta_W)^2 - \frac{5}{3}}_Z + \mathcal{O}\left(\frac{m_\mu^2}{M_Z^2} \log \frac{M_Z^2}{m_\mu^2}\right) + \frac{m_\mu^2}{M_H^2} \int_0^1 dx \frac{2x^2(2-x)}{1-x + \frac{m_\mu^2}{M_H^2}x^2} \right\} \\ = 194.8 \times 10^{-11}, \quad (4.1)$$

where the weak mixing angle is defined by $\sin^2\theta_W = 1 - M_W^2/M_Z^2 \simeq 0.223$, and $G_F \simeq 1.166 \times 10^{-5}$ is the Fermi constant. Notice that the contribution from the Higgs boson, shown in parametric form, is of $\mathcal{O}\left(\frac{G_F m_\mu^2}{\sqrt{2} 4\pi^2} \frac{m_\mu^2}{M_H^2} \ln \frac{M_H^2}{m_\mu^2}\right)$, rather small for the present lower bound on M_H .

The *a priori* possibility that the two-loop electroweak corrections may bring in enhancement factors due to large logarithms, like $\ln(M_Z^2/m_\mu^2) \simeq 13.5$, has motivated a thorough theoretical effort for their evaluation, which has been quite a remarkable achievement.

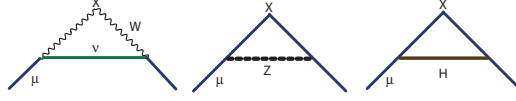


Fig.4 Weak interactions at the one-loop level

It is convenient to separate the two-loop electroweak contributions into two sets: those containing closed fermion loops and the bosonic corrections, which we denote by $a_\mu^{EW(2)}(\text{bos})$. The latter have been evaluated using asymptotic techniques in a systematic expansion in powers of $\sin^2 \theta_W$, where $\log \frac{M_W^2}{m_\mu^2}$ terms, $\log \frac{M_H^2}{M_W^2}$ terms, $\frac{M_W^2}{M_H^2} \log \frac{M_H^2}{M_W^2}$ terms, $\frac{M_W^2}{M_H^2}$ terms, and constant terms are kept. Using $\sin^2 \theta_W = 0.223$ and $50 \text{ GeV} \leq M_H \leq 700 \text{ GeV}$ results in [40, 41, 42]:

$$\begin{aligned} a_\mu^{EW(2)}(\text{bos}) &= \frac{G_F}{\sqrt{2}} \frac{m_\mu^2}{8\pi^2} \times \frac{\alpha}{\pi} (-82.2 \pm 5.9) \\ &= (-22.2 \pm 1.6) \times 10^{-11}. \end{aligned} \quad (4.2)$$

The discussion of the fermionic corrections is more delicate. Because of the $U(1)$ anomaly cancellation between lepton loops and quark loops in the electroweak theory, one cannot separate hadronic from leptonic effects any longer in diagrams like the ones shown in Fig. 5, where a VVA-triangle with two vector currents and an axial-vector current appears. It is therefore appropriate to separate the fermionic corrections into two subclasses. One is the class in Fig. 5, which we denote by $a_\mu^{EW(2)}(l, q)$. The other class is defined by the rest of the diagrams, where quark loops and lepton loops can be treated separately, which we call $a_\mu^{EW(2)}(\text{ferm-rest})$. This latter contribution has been estimated to a very good approximation in ref. [40] with the result,

$$a_\mu^{EW(2)}(\text{ferm-rest}) = \frac{G_F}{\sqrt{2}} \frac{m_\mu^2}{8\pi^2} \frac{\alpha}{\pi} \times (-21 \pm 4), \quad (4.3)$$

where the error here is the one induced by diagrams with Higgs propagators with an allowed Higgs mass in the range $114 \text{ GeV} < M_H < 250 \text{ GeV}$.

Concerning the contributions to $a_\mu^{EW(2)}(l, q)$, it is convenient to treat the three generations separately. The contribution from the third generation can be calculated in a straightforward way using effective field theory techniques [43], because all the fermion masses in the triangle loop are large with respect to the muon mass, with the result [43, 40]:

$$a_\mu^{EW(2)}(\tau, t, b) = \frac{G_F}{\sqrt{2}} \frac{m_\mu^2}{8\pi^2} \frac{\alpha}{\pi} \times (-30.6). \quad (4.4)$$

However, as first emphasized in ref. [43], an appropriate QCD calculation when the quark in the loop of Fig. 5 is a *light quark* should take into account the dominant effects of spontaneous chiral-symmetry breaking. Since this involves the u, d and s quarks, it is convenient to lump together the contributions from the first and second generations. An evaluation of these contributions, which incorporates the QCD long-distance chiral realization [43, 44] as well as perturbative [45] and non-perturbative [44, 45] short-distance constraints, gives the result

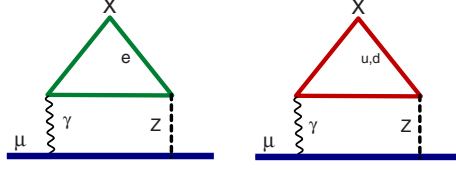


Fig.5 Two-loop electroweak diagrams generated by the $\gamma\gamma Z$ -Triangle. There are similar diagrams corresponding to the μ, c, s and τ, t, b generations.

$$a_{\mu}^{EW(2)}(e, \mu, u, d, s, c) = \frac{G_F}{\sqrt{2}} \frac{m_{\mu}^2}{8\pi^2} \frac{\alpha}{\pi} \times (-24.6 \pm 1.8). \quad (4.5)$$

From the theoretical point of view, this calculation has revealed surprising properties concerning the *non-anomalous* component of the VVA-triangle [46], resulting in a new set of *non-renormalization theorems* in perturbation theory [46, 47].

Putting together the partial two-loop results discussed above, one finally obtains for the overall electroweak contribution the value

$$\begin{aligned} a_{\mu}^{EW} &= a_{\mu}^{EW(1)} + \frac{G_F}{\sqrt{2}} \frac{m_{\mu}^2}{8\pi^2} \left(\frac{\alpha}{\pi}\right) [-158.4(7.1)(1.8)] \\ &= 152(2)(1) \times 10^{-11}, \end{aligned} \quad (4.6)$$

where the first error is essentially due to the Higgs mass uncertainty, while the second comes from hadronic uncertainties in the VVA-loop evaluation. The overall result shows indeed that the two-loop correction represents a sizeable reduction of the one-loop result by an amount of 22%. An evaluation of the electroweak three-loop leading terms of $\mathcal{O} \left[\frac{G_F}{\sqrt{2}} \frac{m_{\mu}^2}{8\pi^2} \left(\frac{\alpha}{\pi}\right)^2 \ln \frac{M_Z}{m_{\mu}} \right]$, using renormalization group arguments [48, 45], shows that higher order effects are negligible [$\mathcal{O}(10^{-12})$] for the accuracy needed at present.

5. Summary

CONTRIBUTION	RESULT IN 10^{-11} UNITS
QED (leptons)	$116\,584\,718.09 \pm 0.14 \pm 0.04\alpha$
HVP(lo)[e^+e^-]	$6\,873 \pm 42_{\text{exp}} \pm 19_{\text{rad}} \pm 7_{\text{QCD}}$
HVP(ho)	$-97.9 \pm 0.9_{\text{exp}} \pm 0.3_{\text{rad}}$
HLxL	105 ± 26
EW	$152 \pm 2 \pm 1$
Total SM	$116\,591\,750 \pm 53$

Table 2 collects the various Standard Model contributions to a_{μ} which we have discussed. Notice that the largest error at present is the one from the lowest order hadronic vacuum polarization

contribution. Adding experimental and theoretical errors in quadrature gives a total

$$a_{\mu}^{\text{SM}} = (116\,591\,750 \pm 53) \times 10^{-11}, \quad (5.1)$$

with an overall error slightly smaller than the one in the experimental determination in Eq. (1.2). The comparison between these two numbers shows an intriguing 3.6σ discrepancy. However, if instead of the HVP(lo)[e^+e^-] value one uses the τ -data determination in Eq. (3.4), the discrepancy is then reduced to a 2.2σ deviation. We are eagerly awaiting for the new BaBar data to clarify this situation.

References

- [1] G.W. Bennett *et al* [Muon ($g-2$) Collaboration], Phys.Rev. **D73** 072003 (2006).
- [2] J.P. Miller, E. de Rafael and B.L. Roberts, Rep. Prog. Phys. **70** 795 (2007).
- [3] F. Jegerlehner and A. Nyffeler, arXiv:0902.3360v1 [hep-ph].
- [4] J. Schwinger, Phys. Rev. **76** 790 (1949).
- [5] A. Petermann, Helv. Phys. Acta **30** 407 (1957); Nucl. Phys. **5** 677 (1958).
- [6] C.M. Sommerfield, Phys. Rev. **107** 328 (1957); Ann. Phys. (N.Y.) **5** 26 (1958).
- [7] S. Laporta and E. Remiddi, Phys. Lett. **B379** 283 (1996).
- [8] T. Aoyama, M. Hayakawa, T. Kinoshita and M. Nio, Phys. Rev. Lett. **99** 110406 (2007).
- [9] D. Hanneke, S. Fogwell and G. Gabrielse, Phys. Rev. Lett. **100** 120801 (2008).
- [10] S. Laporta, Nuovo Cim. **A106** 675 (1993).
- [11] S. Laporta and E. Remiddi, Phys. Lett. **B301** 440 (1993).
- [12] M. Passera, J.Phys.G. **31** R75 (2005).
- [13] T. Kinoshita and M. Nio, Phys. Rev. **D70** 113001 (2004).
- [14] T. Kinoshita and M. Nio, Phys. Rev. **D73** 053007 (2006).
- [15] S. Friot, D. Greynat and E. de Rafael, Phys. Lett. **B628** 73 (2005).
- [16] J.-Ph. Aguilar, D. Greynat and E. de Rafael, Phys. Rev. **D77** 093010 (2008).
- [17] B.E. Lautrup and E. de Rafael, Nucl. Phys. **B70** 317 (1974).
- [18] A.I. Kataev, Phys. Rev. **D74** 073011 (2006).
- [19] J.-Ph. Aguilar, PhD Thesis, (2008).
- [20] J.-Ph. Aguilar and E. de Rafael, *to be published*.
- [21] C. Bouchiat and L. Michel, J. Phys. Radium **22** 121 (1961).
- [22] M. Gourdin and E. de Rafael, Nucl. Phys. **B10** 667 (1969).
- [23] J.S. Bell and E. de Rafael, Nucl.Phys. **B11** 611 (1969).
- [24] Michel Davier, Chapter 8 in *Lepton Moments*, to be published by World Scientific Review Volume.
- [25] J. Calmet, S. Narison, M. Perrottet and E. de Rafael, Phys. Lett. **B61** 283 (1975).

- [26] S. Brodsky and E. de Rafael, Phys. Rev. **168** 1620 (1968).
- [27] B.E. Lautrup and E. de Rafael, Phys. Rev. **174** 1835 (1968).
- [28] R. Barbieri and E. Remiddi, Nucl. Phys. **B90** 997 (1975).
- [29] K. Hagiwara, A.D. Martin, D. Nomura and T. Teubner, Phys. Lett. **B649** 173 (2007).
- [30] M. Knecht, A. Nyffeler, M. Perrottet and E. de Rafael, Phys. Rev. Lett. **88** 071802 (2002).
- [31] M. Knecht and A. Nyffeler, Phys. Rev. **D65** 073034 (2002).
- [32] M. Ramsey-Musolf and M. B. Wise, Phys. Rev. Lett. **89** 041601 (2002).
- [33] M. Hayakawa and T. Kinoshita, Phys. Rev. **D66** 073034 (2002) (Erratum).
- [34] J. Bijnens, E. Pallante and J. Prades, Nucl. Phys. **B626** 410 (2002).
- [35] K. Melnikov and A. Vainshtein, Phys. Rev. **D70** 113006 (2004).
- [36] A. Nyffeler, arXiv:0901.1172v1 [hep-ph].
- [37] E. de Rafael, Phys.Lett. **B322** 239 (1994).
- [38] J. Prades, E. de Rafael and A. Vainshtein, *Glasgow White Paper*, arXiv:0901.0306v1 [hep-ph]. See also Chapter 9 in *Lepton Moments*, to be published by World Scientific Review Volume.
- [39] W.A. Bardeen, R. Gastmans and B.E. Lautrup, Nucl. Phys. **B46** 315 (1972).
- [40] A. Czarnecki, A. Krause and W. Marciano, Phys. Rev. **D52** 2619 (1995); Phys. Rev. Lett. **76** 3267 (1996).
- [41] S. Heinemeyer, D.Stöckinger and G. Weiglein, Nucl. Phys. **B699** 103 (2004).
- [42] T. Gribouk and A. Czarnecki, Phys. Rev. **D72** 053016 (2005).
- [43] S. Peris, M. Perrottet and E. de Rafael, JHEP **05** 011 (1998).
- [44] M. Knecht, S. Peris, M. Perrottet and E. de Rafael, JHEP **0211** (2002) 003.
- [45] A. Czarnecki, W.J. Marciano and A. Vainshtein, Phys. Rev. **D67** 073006 (2003) [Erratum-ibid. **D73** 119901 (2006)].
- [46] A. Vainshtein, Phys. Lett. **B569** (2003) 187.
- [47] M. Knecht, S. Peris, M. Perrottet and E. de Rafael, JHEP **0403** 035 (2004).
- [48] G. Degradi and G.F. Giudice, Phys. Rev. **D58** 053007 (1998).